To What Extent Do External Fields and Vibrational and Isotopic Effects Influence NMR Coupling Constants Across Hydrogen Bonds? Two-Bond Cl−N Spin−Spin Coupling Constants ($^{2h}J_{Cl-N}$) in Model ClH:NH_3 Complexes

Janet E. Del Bene*,†,‡ and Meredith J. T. Jordan§

Department of Chemistry, Youngstown State University, Youngstown, Ohio 44555, Quantum Theory Project, University of Florida, Gainesville, Florida 32611, and School of Chemistry, University of Sydney, Sydney, NSW 2006 Australia

Received: February 6, 2002; In Final Form: March 22, 2002

EOM-CCSD calculations are performed to evaluate two-bond $^{35}Cl-^{15}N$ spin−spin coupling constants ($^{2h}J_{Cl-N}$) for ClH:NH_3 complexes. Coupling constants for structures in external electric fields of 0.0000, 0.0055, and 0.0150 au are investigated as models for complexes with traditional, proton-shared, and ion-pair hydrogen bonds. Two-dimensional coupling constant surfaces are constructed at these field strengths in the NH and ClH distances, and expectation values, $\langle^{2h}J_{Cl-N}\rangle$, are calculated for ground and selected excited vibrational states of the dimer- and proton-stretching modes from the corresponding anharmonic wave functions. Single-point values, $^{2h}J_{Cl-N}$, are also calculated at the equilibrium geometry for each field strength and at the geometry corresponding to the ground-state expectation values of the NH and ClH bond lengths. Coupling constants evaluated in the presence of the electric field are referred to as explicit $\langle^{2h}J_{Cl-N}\rangle$ and $^{2h}J_{Cl-N}$. Implicit $\langle^{2h}J_{Cl-N}\rangle$ and $^{2h}J_{Cl-N}$ are evaluated from the zero-field coupling constant surface using the geometries and vibrational wave functions (for expectation values) from the 0.0055 and 0.0150 au surfaces. Both $\langle^{2h}J_{Cl-N}\rangle$ and $^{2h}J_{Cl-N}$ are larger when computed in the presence of the external field, and exhibit maximum (absolute) values for proton-shared hydrogen bonds. $^{2h}J_{Cl-N}$ computed at the equilibrium geometry may be significantly different from $\langle^{2h}J_{Cl-N}\rangle_{0,0}$ and $^{2h}J_{Cl-N}$ computed at the ground-state geometry, but whether the equilibrium or the ground-state coupling constant is greater depends on hydrogen bond type. Similarly, isotopic substitution of D for the hydrogen-bonded H also changes both $\langle^{2h}J_{Cl-N}\rangle$ and $^{2h}J_{Cl-N}$, but which isotopomer has the larger coupling constant also depends on hydrogen bond type. Thermal vibrational averaging of ClH:NH_3 and ClD:NH_3 Cl−N spin−spin coupling constants at temperatures below 300 K has essentially no effect.

Introduction

Recent studies of NMR two-bond spin−spin coupling constants ($^{2h}J_{X-Y}$) across X−H−Y hydrogen bonds have suggested that structural data and information about hydrogen bond type can be obtained from $^{2h}J_{X-Y}$.[1−23] Our work in this area has focused on systematic ab initio EOM-CCSD studies of spin−spin coupling constants across hydrogen bonds.[15−23] In these studies, we have addressed fundamental questions concerning the dependence of $^{2h}J_{X-Y}$ on X−Y distances, the nature of the atoms X and Y, the bonding at these atoms, the charge on the complex, the orientation of the hydrogen-bonded pair, and the hydrogen bond type.

As part of a continuing effort to better characterize and understand coupling constants, we have embarked on a detailed study of two-bond coupling constants across the hydrogen bond in a model complex, ClH:NH_3. Despite the fact that there are no experimental measurements of $^{35}Cl-^{15}N$ coupling constants (the chlorine atom has a nuclear quadrupole, which results in very fast spin relaxation times), the ClH:NH_3 complex is attractive from a theoretical viewpoint, because it is possible to change the nature of the Cl−H−N hydrogen bond by applying external electric fields of varying strengths along the hydrogen-bonding axis.[24] At zero-field, ClH:NH_3 is stabilized by a traditional Cl−H···N hydrogen bond. As the field increases to 0.0055 au, the hydrogen bond becomes a proton-shared Cl···H···N bond which is close to quasisymmetric. At the higher field of 0.0150 au, the hydrogen bond has $Cl^-\cdots{}^+H-N$ ion-pair character.

In the present work, we will address the following fundamental questions, each of which is relevant to the interpretation of experimental data.

1. How do coupling constants vary with hydrogen bond type?

2. How do Cl−N coupling constants computed for equilibrium structures compare with those evaluated at ground-state geometries, that is, geometries corresponding to the ground-state expectation values of the coordinates, and with coupling constants evaluated as expectation values for ground and excited vibrational states?

3. To what extent does thermal vibrational averaging over dimer- and proton-stretching excited states change coupling constants?

4. How do coupling constants evaluated as explicit and implicit functions of the strength of an external field compare? Here we use explicit and implicit to mean that the coupling constant is calculated in the presence or absence of the electric field, respectively. For both calculations, the geometries and wave functions (for expectation values) have been calculated in the presence of the field.

* To whom correspondence should be addressed.
† Youngstown State University.
‡ University of Florida.
§ University of Sydney.

10.1021/jp020348b CCC: $22.00
Published on Web 05/02/2002

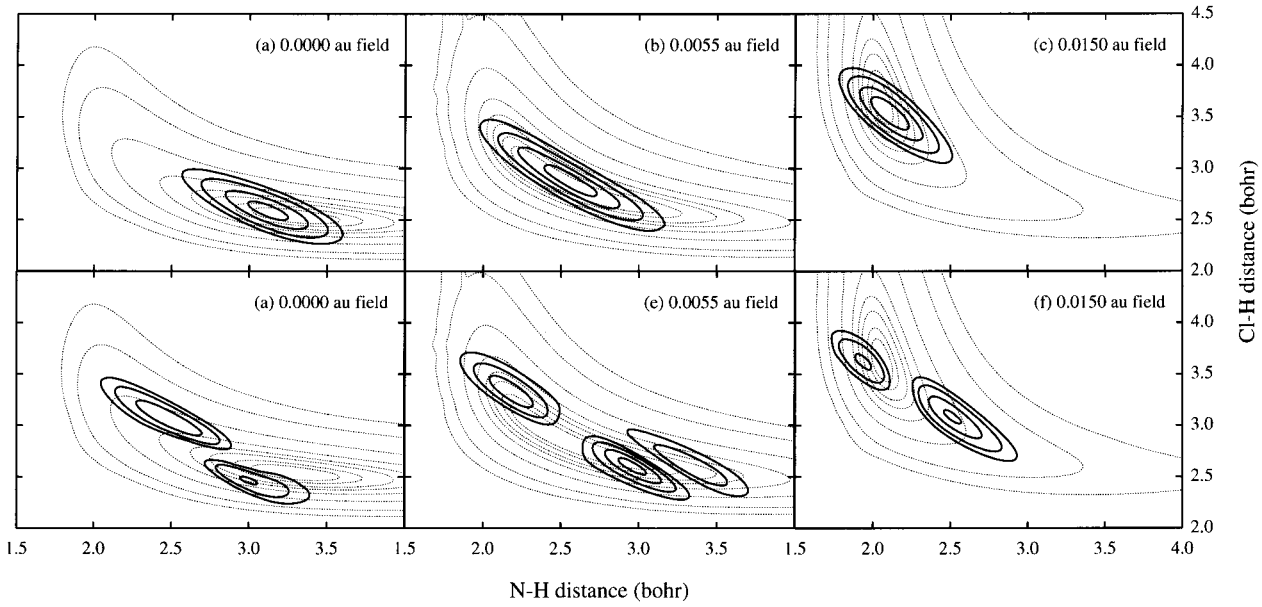

Figure 1. Square of the ground-state wave functions (upper plots) and the wave functions for the $\upsilon = 1$ state of the proton-stretching mode (lower plots) superimposed on the potential energy surfaces at field strengths of 0.0000, 0.0055, and 0.0150 au. Contour values are at 0.0005, 0.001, 0.002, 0.003, 0.005, 0.01, 0.02, and 0.03 au above the global minimum. Plots for the ground-state wave functions and the $\upsilon = 1$ state of the proton-stretching vibration at zero-field are taken from ref 24.

5. What effect does isotopic substitution of D for the hydrogen-bonded H have on Cl−N coupling constants?

Methods of Calculation

In a previous study,[24] two-dimensional potential energy surfaces at second-order Møller−Plesset perturbation theory (MP2)[25−28] with the aug′-cc-pVDZ basis set[29,30] were generated for ClH:NH_3 by freezing the NH_3 coordinates at their equilibrium values and then varying the Cl−H and N−H distances. Results at nonzero-field strengths were similarly obtained by applying an external field along the Cl−H−N direction of the complex and varying the Cl−H and N−H distances. The ab initio data points were generated to cover the most chemically relevant areas of the potential surfaces, including those regions associated with traditional, proton-shared, and ion-pair hydrogen bonds. Details of the construction of the global surfaces and the calculation of the one- and two-dimensional anharmonic vibrational eigenfunctions and eigenvalues for both ClH:NH_3 and ClD:NH_3 are reported in previous papers.[24,31]

Two-dimensional Cl−N spin−spin coupling constant surfaces were also generated in the Cl−H and N−H coordinates. The $^{2h}J_{Cl-N}$ surfaces were approximated by the Fermi-contact term, because it had been demonstrated previously that the other terms contributing to the spin−spin coupling constant (paramagnetic spin−orbit, diamagnetic spin−orbit, and spin dipole) are negligible.[17] The ab initio data points were obtained from equation-of-motion coupled cluster (EOM-CCSD) theory using the CI-like approximation.[32] For these calculations, a qzp basis set was used on Cl and N, qz2p was used on the hydrogen-bonded proton,[33] and Dunning's cc-pVDZ basis[29,30] was used on the NH_3 hydrogens. The ab initio grid was generated by varying the Cl−N distance from 2.70 to 3.30 Å in increments of 0.05 Å. At each Cl−N distance, the Cl−H distance was set to 1.05 Å and incremented in steps of 0.05 Å until the N−H distance decreased to 0.95 Å. The global coupling constant surfaces were constructed in a manner analogous to the potential surfaces.[24] This procedure involved interpolating the grid of ab initio data and using polynomial extrapolations to obtain the global property surface. The sensitivity of the results to the order of the polynomial extrapolations has been investigated. Coupling constant surfaces were constructed at zero-field and at field strengths of 0.0055 and 0.0150 au.

The two-dimensional anharmonic vibrational wave functions obtained at field strengths of 0.0000, 0.0055, and 0.0150 au were used to obtain expectation values, $\langle ^{2h}J_{Cl-N}\rangle$, of coupling constants in the ground and excited states of the dimer- and proton-stretching modes from the $^{2h}J_{Cl-N}$ surface at zero-field. Coupling constants obtained in this way are referred to as implicit $\langle ^{2h}J_{Cl-N}\rangle$. The vibrational wave functions obtained from the 0.0055 and 0.0150 au potential energy surfaces were also used to compute $\langle ^{2h}J_{Cl-N}\rangle$ from the corresponding 0.0055 and 0.0150 au field coupling constant surfaces. Coupling constants obtained in this way are referred to as explicit $\langle ^{2h}J_{Cl-N}\rangle$. Similarly, explicit and implicit values of $^{2h}J_{Cl-N}$ have been obtained from single-point calculations at equilibrium geometries and at the geometry corresponding to the ground-state expectation values of Cl−N and Cl−H (or Cl−D) distances.

Thermally averaged coupling constants were computed at 100, 150, 200, and 298 K. All excited vibrational states up to and including the first state with an anharmonic frequency greater than 2000 cm^{-1} were included in these calculations, ensuring convergence to better than 0.001 Hz.

The coupling constant calculations were performed using the ACES II program.[34] All of the calculations reported in this paper were carried out on the Cray SV1 computer at the Ohio Supercomputer Center and on the computing facilities at the University of Sydney.

Results and Discussion

Insight into the variation of coupling constants computed at equilibrium and in ground and excited vibrational states of ClH:NH_3 at 0.0000, 0.0055, and 0.0150 au fields may be gained by first examining the nature of the potential surfaces at these fields and the associated vibrational wave functions. Figure 1 presents the square of the wave functions for the ground states and first-excited states of the proton-stretching mode superimposed on the potential surfaces. The equilibrium and ground-state expectation values of Cl−N, Cl−H, and Cl−D distances

TABLE 1: Cl−N, Cl−H, and Cl−D Distances (Å) at Equilibrium (R_e) and in the Ground ($R_{0,0}$) and First-Excited Dimer- ($R_{1,0}$) and Proton-Stretching ($R_{0,1}$) States as a Function of Field Strength (au)[a]

	ClH:NH_3		ClD:NH_3	
	Cl−N	Cl−H	Cl−N	Cl−D
		Field = 0.0000		
R_e	3.080	1.341	3.080	1.341
$R_{0,0}$	3.016	1.392	3.041	1.374
$R_{1,0}$	3.054	1.389	3.073	1.373
$R_{0,1}$	2.944	1.558	2.940	1.480
		Field = 0.0055		
R_e	2.832	1.575	2.832	1.575
$R_{0,0}$	2.870	1.546	2.878	1.538
$R_{1,0}$	2.920	1.510	2.934	1.479
$R_{0,1}$	2.972	1.526	2.963	1.515
		Field = 0.0150		
R_e	3.004	1.917	3.004	1.917
$R_{0,0}$	2.988	1.857	2.996	1.878
$R_{1,0}$	2.982	1.857	3.024	1.911
$R_{0,1}$	2.961	1.707	2.960	1.760

[a] Data for ClH:NH_3 and ClD:NH_3 taken from refs 24 and 31, respectively.

at each field strength are given in Table 1 for both ClH:NH_3 and ClD:NH_3. Because the spin−spin coupling constant has previously been shown to be directly dependent on the Cl−N distance,[17] it is useful to see how this distance varies as the field strength and the vibrational state change. At zero-field, the minimum on the surface is located in the region of the traditional hydrogen bond, and the ground-state wave function is centered in this region. However, it is slightly displaced toward the proton-shared region of the surface. As a result, the ground-state expectation value of the Cl−N distance is shorter than the equilibrium distance. As the field increases, the minimum moves toward the proton-shared region of the surface. At a field of 0.0055 au, the minimum is very broad, and the complex has a proton-shared hydrogen bond. At this field, the ground-state wave function is delocalized. The equilibrium Cl−N distance is shorter than at the other two fields and is also shorter than the expectation value of the Cl−N distance in the ground vibrational state. As the field further increases to 0.0150 au, the minimum on the potential surface becomes more sharply defined, and a wave function that describes a hydrogen-bonded ion pair is found. This wave function is now more localized and is slightly displaced toward the proton-shared region of the surface. As in the zero-field case, the expectation value of the Cl−N distance in the ground vibrational state is shorter than the equilibrium distance.

The squares of the vibrational wave functions for the $v = 1$ state of the proton-stretching mode are also shown in Figure 1. At zero-field, the wave function extends into the proton-shared region of the surface, with the result that the expectation value of the Cl−N distance in the $v = 1$ state of the proton-stretching mode is significantly shorter than both the equilibrium and the ground-state distances. At a field of 0.0055 au, the excited-state wave function is displaced from the proton-shared region, extending into the traditional and ion-pair regions of the surface. The expectation value of the Cl−N distance is significantly greater than the equilibrium and ground-state distances. (It should be noted that the wave function for this state has an extra node. This node arises from Fermi resonance between the $v = 1$ state of the proton-stretching mode and the $v = 3$ state of the dimer-stretching mode. The wave function for the dimer $v = 3$ excited state is shown in Figure 2. On the basis of these wave functions, we have identified the wave function in Figure 1e as that corresponding to the $v = 1$ proton-stretching state. A consequence of the mixing between these two states will be apparent later when $\langle {}^{2h}J_{Cl-N}\rangle$ for the two states is discussed.) Finally, at a field of 0.0150 au, the wave function for the $v = 1$ state of the proton-stretching mode is displaced toward the proton-shared region of the surface. This leads to a decrease in the expectation value of the Cl−N distance in the excited state of the proton-stretching vibration relative to the equilibrium and ground-state distances.

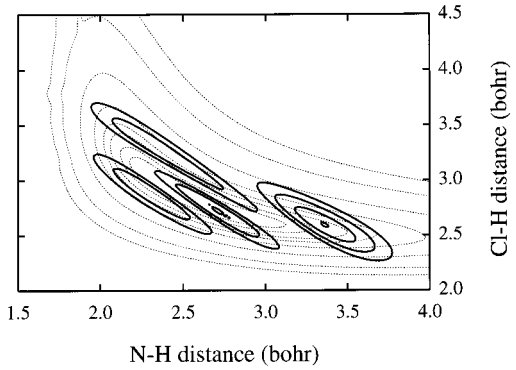

Figure 2. Square of the wave function for the $v = 3$ state of the dimer-stretching mode superimposed on the 0.0055 au potential surface. Contour values are the same as in Figure 1.

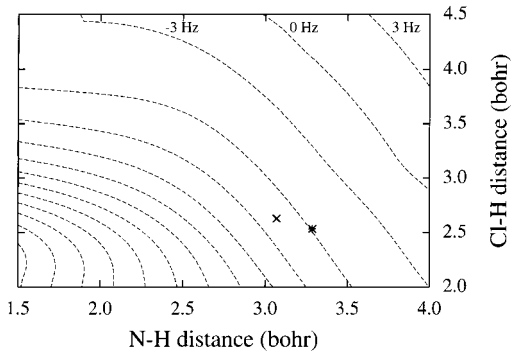

Figure 3. $^{2h}J_{Cl-N}$ surface at zero-field. Contours are in increments of 3 Hz, and values of selected contours are indicated. The equilibrium geometry is marked with an (*), and the geometry corresponding to the expectation values of the Cl−N and Cl−H distances in the ground vibrational state is marked with an (×).

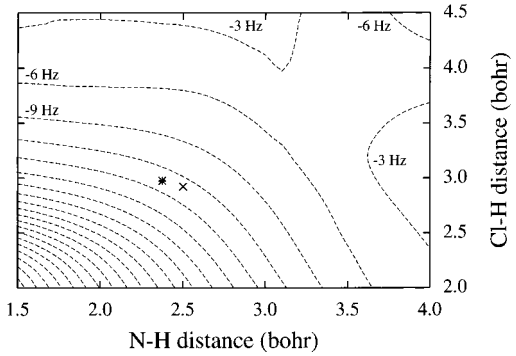

Figure 4. $^{2h}J_{Cl-N}$ surface at a field of 0.0055 au. Contours are in increments of 3 Hz, and values of selected contours are indicated. Equilibrium and ground-state geometries are marked as in Figure 3.

$^{2h}J_{Cl-N}$ Property Surfaces. As noted above, global $^{2h}J_{Cl-N}$ property surfaces have been constructed analogously to the potential energy surfaces,[24] and the surfaces at 0.0000, 0.0055, and 0.0150 au are illustrated in Figures 3−5, respectively. These surfaces were constructed using bicubic spline interpolation of the ab initio data grid and a linear extrapolation outside the ab

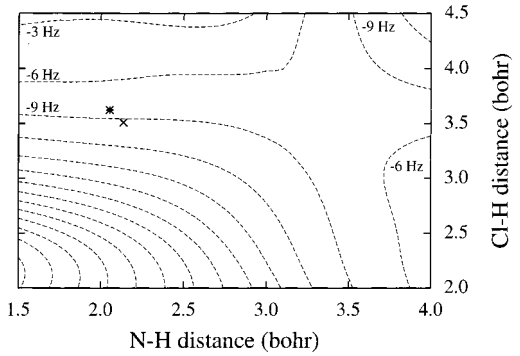

Figure 5. $^{2h}J_{Cl-N}$ surface at a field of 0.0150 au. Contours are in increments of 3 Hz, and values of selected contours are marked for reference. Equilibrium and ground-state geometries are marked as in Figure 3.

TABLE 2: ClH:NH_3 Vibrational Frequencies (v, cm^{-1}) and Expectation Values of the Cl−N Spin−Spin Coupling Constants ($\langle^{2h}J_{Cl-N}\rangle$, Hz) as a Function of Vibrational State and $^{2h}J_{Cl-N}$ Property Surface Extrapolation Procedure at Zero-Field

state[a]	frequency	$\langle^{2h}J_{Cl-N}\rangle^b$	$\langle^{2h}J_{Cl-N}\rangle^c$
(0,0)		−7.52	−7.52
(1,0)	201.6	−7.04	−7.04
(2,0)	400.6	−6.57	−6.58
(3,0)	596.5	−6.18	−6.22
(4,0)	790.6	−5.85	−5.94
(5,0)	983.0	−5.53	−5.72
(6,0)	1172.8	−5.19	−5.52
(7,0)	1358.6	−4.84	−5.35
(8,0)	1538.9	−4.64	−5.34
(9,0)	1716.4	−4.15	−5.10
(10,0)	1887.5	−3.93	−5.06
(11,0)	2056.2	−3.60	−4.86
(0,1)	1567.0	−9.28	−9.31
(1,1)	1931.6	−8.68	−8.71

[a] The notation (i,j) indicates i quanta of energy in the dimer-stretching mode and j quanta of energy in the proton-stretching mode. [b] Computed from the coupling constant surface obtained using linear extrapolation. [c] Computed from the coupling constant surface obtained using quadratic extrapolation.

initio grid; no attempt to fit a functional form to these data has been made. However, the choice of extrapolation procedure is arbitrary. Ideally, the ab initio grid covers the regions of configuration space sampled by the wave functions of interest, and expectation values of the coupling constant over these wave functions are insensitive to the extrapolation procedure. This has been tested by using either linear or quadratic extrapolation to obtain the global coupling constant surfaces. Table 2 lists the zero-field two-dimensional anharmonic frequencies and $\langle^{2h}J_{Cl-N}\rangle$ for the ground and excited dimer- and proton-stretching vibrational states, up to and including the first state with a frequency above 2000 cm^{-1}, obtained using either linear or quadratic extrapolation. It is evident from Table 2 that $\langle^{2h}J_{Cl-N}\rangle$ in the ground state, the lower-energy excited states of the dimer-stretching mode, and the first excited state of the proton-stretching mode are insensitive to the extrapolation procedure. The higher energy dimer-stretching states, however, do show a dependence on the extrapolation procedure. In these higher energy states, the wave functions extend beyond the configuration space spanned by the ab initio data points, and consequent errors are introduced. It is interesting to note that when the vibrational wave functions are more symmetrically located on the surface, as they are at a field strength of 0.0055 au (See Figure 1), then the differences between $\langle^{2h}J_{Cl-N}\rangle$ obtained using linear and quadratic extrapolations are much smaller than in the zero-field case, not exceeding 0.15 Hz in any vibrational state up to and including the first state with a frequency above 2000 cm^{-1}. Regardless, because differences in $\langle^{2h}J_{Cl-N}\rangle$ occur only for the higher energy states that are not significantly populated even at 300 K, thermally averaged coupling constants below 300 K computed from the two data sets are essentially identical. Subsequent calculations were carried out using coupling constant surfaces constructed from linear extrapolation.

The vagaries of using an extrapolation procedure to produce a global property surface are also apparent in Figures 4 and 5. As the Cl−N distance in ClH:NH_3 increases, the value of the coupling constant should eventually go to zero. The features observed at large Cl−N distances for the coupling constant surfaces at fields of 0.0055 and 0.0150 au are unphysical and are an artifact of the extrapolation procedure. However, because the vibrational wave functions for the ground and lower-energy vibrational states do not extent into this region, these features have no effect on the calculated $\langle^{2h}J_{Cl-N}\rangle$ for these states or on the thermally averaged coupling constants for the ground state.

A comparison of the coupling constant surfaces at fields of 0.0000, 0.0055, and 0.0150 au plotted in Figures 3−5, respectively, shows that the contours on the zero-field surface are not as closely spaced as on the other two surfaces. This means that $^{2h}J_{Cl-N}$ will be least sensitive to changes in Cl−H and Cl−N distances on this surface. In addition, the value of the coupling constant on the zero-field surface at a given geometry is less (in absolute value) than the value of the coupling constant at that geometry on the non-zero-field surfaces. Thus, implicit values of $^{2h}J_{Cl-N}$ underestimate explicit values. Finally, it should be noted that the contours on the 0.0055 au surface, the field associated with the proton-shared hydrogen bond, are the most closely spaced. This leads to a greater sensitivity of $^{2h}J_{Cl-N}$ on Cl−N and Cl−H distances at this field strength.

The equilibrium and ground-state geometries at fields strengths of 0.0000, 0.0055, and 0.0150 au are reported in Table 1. In Figures 3−5, the equilibrium geometry on each coupling constant surface has been indicated by an asterisk, and the geometry corresponding to the ground-state expectation values of the N−H and Cl−H distances has been indicated by an "×". From the relative positions of these indicators, it is easy to see how single point calculations of $^{2h}J_{Cl-N}$ at equilibrium and ground-state geometries will compare at a given field strength. At zero-field and at a field of 0.0150 au, the value of $^{2h}J_{Cl-N}$ at equilibrium will be less than the ground-state value, whereas at a field of 0.0055 au, the value of $^{2h}J_{Cl-N}$ at equilibrium will be greater. (The computed Cl−N spin−spin coupling constants have negative signs. In subsequent sections of this paper, changes in coupling constants will be described relative to the absolute value of the coupling constants.)

$^{2h}J_{Cl-N}$ at Equilibrium and Ground-State Geometries and $\langle^{2h}J_{Cl-N}\rangle$ in Ground and Excited Vibrational States. The single-point values of $^{2h}J_{Cl-N}$ for ClH:NH_3 and ClD:NH_3 computed at the equilibrium geometry, the geometry corresponding to the ground-state expectation values of the Cl−N and Cl−H distances, and $\langle^{2h}J_{Cl-N}\rangle$ calculated for the ground vibrational state, the first four excited states of the dimer-stretching mode, and the first-excited state of the proton-stretching mode are reported in Table 3 as a function of external electric field strength. At the equilibrium geometry at zero-field, $^{2h}J_{Cl-N}$ has a value of −5.9 Hz. Relative to the equilibrium value, the ground-state expectation value of $^{2h}J_{Cl-N}$ ($\langle^{2h}J_{Cl-N}\rangle_{0,0}$) in ClH:$NH_3$ increases to −7.5 Hz. This increase is a consequence of the distance dependence of the Fermi-contact term, which increases as the Cl−N distance decreases. This has been

TABLE 3: ClH:NH$_3$ and ClD:NH$_3$ Vibrational Frequencies (υ, cm^{-1}) and Expectation Values of the Cl−N Spin−Spin Coupling Constant ($\langle^{2h}J_{Cl-N}\rangle$, Hz) as a Function of Vibrational State and Field Strength

ClH:NH$_3$			ClD:NH$_3$		
state[a]	υ	$\langle^{2h}J_{Cl-N}\rangle$[d]	state[a]	υ	$\langle^{2h}J_{Cl-N}\rangle$[d]
		0.0000 au Field			
(0,0)		−7.52	(0,0)		−6.95
(1,0)	201.6	−7.04	(1,0)	191.6	−6.65
(2,0)	400.6	−6.57	(2,0)	379.6	−6.34
(3,0)	596.5	−6.18	(3,0)	565.9	−6.04
(4,0)	790.6	−5.85	(4,0)	752.2	−5.75
(0,1)	1567.0	−9.28	(0,1)	1265.6	−9.38
$^{2h}J_{Cl-N}$(eq)[b]		−5.88			−5.88
$^{2h}J_{Cl-N}$(gs)[c]		−7.46			−6.83
		0.0055 au Field			
(0,0)		−12.09 (−10.68)	(0,0)		−12.34 (−10.90)
(1,0)	371.7	−11.42(−9.95)	(1,0)	336.5	−11.10 (−9.58)
(2,0)	676.8	−10.40 (−8.96)	(2,0)	582.1	−10.96 (−9.64)
(3,0)	966.6	−10.38 (−9.04)	(3,0)	880.9	−9.73 (−8.31)
(4,0)	1214.8	−8.89 (−7.53)	(4,0)	1155.9	−8.89 (−7.53)
(0,1)	936.1	−9.69 (−8.41)	(0,1)	663.3	−10.09 (−8.71)
$^{2h}J_{Cl-N}$(eq)[b]		−13.53 (−12.19)			−13.53 (−12.19)
$^{2h}J_{Cl-N}$(gs)[c]		−13.02 (−11.51)			−12.88 (−11.34)
		0.0150 au Field			
(0,0)		−9.45 (−7.81)	(0,0)		−9.08 (−7.59)
(1,0)	274.4	−8.99 (−7.48)	(1,0)	257.9	−8.68 (−7.30)
(2,0)	538.7	−8.57 (−7.18)	(2,0)	507.3	−8.30 (−7.02)
(3,0)	791.2	−8.12 (−6.85)	(3,0)	745.9	−7.85 (−6.70)
(4,0)	1029.0	−7.62 (−6.50)	(4,0)	968.7	−7.30 (−6.31)
(0,1)	1781.5	−11.58 (−8.78)	(0,1)	1431.2	−11.06 (−8.69)
$^{2h}J_{Cl-N}$(eq)[b]		−8.23 (−7.05)			−8.23 (−7.05)
$^{2h}J_{Cl-N}$(gs)[c]		−9.36 (−7.83)			−8.96 (−7.54)

[a] The notation (i,j) indicates i quanta of energy in the dimer-stretching mode and j quanta of energy in the proton-stretching mode. [b] The single-point coupling constant evaluated at the equilibrium geometry. [c] The single-point coupling constant evaluated at the expectation values of the Cl−N, Cl−H, and Cl−D distances in the ground state. [d] The values of the coupling constants given in these tables are explicit values obtained from the coupling constant surface using the geometries and wave functions (for expectation values) at that field. The values in parentheses are implicit values obtained using the appropriate geometries and vibrational wave functions for expectation values at the given field but evaluated from the coupling constant surface at zero-field.

observed previously[17] and can be clearly seen in Figure 3. The expectation value of the Cl−N distance in the ground vibrational state is shorter than the equilibrium Cl−N distance, as evident from Table 1. Moreover, decreasing Cl−N distance and increasing Cl−H distance are suggestive of increased proton-shared character, which is also associated with larger two-bond spin−spin coupling constants.[16,17,20,21]

At zero-field, $\langle^{2h}J_{Cl-N}\rangle$ for the first excited state of the dimer-stretching mode decreases relative to the ground state as the expectation value of the Cl−N distance increases. This is apparent from Tables 1 and 3, which show that $\langle^{2h}J_{Cl-N}\rangle$ in the first excited state of the dimer stretching mode of ClH:NH$_3$ decreases from −7.5 to −7.0 Hz as the expectation value of the Cl−N distance increases from 3.016 to 3.054 Å. $\langle^{2h}J_{Cl-N}\rangle$ continues to decrease as the higher energy dimer-stretching modes are excited. In contrast, $\langle^{2h}J_{Cl-N}\rangle$ for the first excited state of the proton-stretching mode is −9.3 Hz, compared to the ground-state value of −7.5 Hz. This rather dramatic increase correlates with a decrease in the expectation value of the Cl−N distance to 2.944 Å and an increase in the expectation value of the Cl−H distance to 1.558 Å. The greater proton-shared character of the hydrogen bond in the first excited state of the proton-stretching mode compared to the ground vibrational state leads to a greater $\langle^{2h}J_{Cl-N}\rangle$.

The changes observed in the zero-field $\langle^{2h}J_{Cl-N}\rangle$ for ClH:NH$_3$ are also seen for ClD:NH$_3$. The value of $^{2h}J_{Cl-N}$ at the equilibrium geometry is −5.9 Hz, whereas $\langle^{2h}J_{Cl-N}\rangle$ for the ground vibrational state is −7.0 Hz. $\langle^{2h}J_{Cl-N}\rangle$ decreases further in the excited states of the dimer stretching mode but, again, increases in the first excited state of the proton-stretching mode. These changes are related to changes in Cl−N and Cl-D distances, as seen in Table 1. Moreover, $\langle^{2h}J_{Cl-N}\rangle$ in the ground vibrational state of ClD:NH$_3$ is less than it is in the ground state of ClH:NH$_3$. This correlates with the longer Cl−N and shorter Cl-D distances in ClD:NH$_3$ relative to ClH:NH$_3$, as evident from Table 1.

Coupling constants for ClH:NH$_3$ and ClD:NH$_3$ at a field of 0.0055 au are also reported in Table 3. At this field strength, the hydrogen bond is proton-shared and close to quasisymmetric. As a result, $^{2h}J_{Cl-N}$ calculated at the equilibrium geometry has its largest value of −13.5 Hz. In contrast to the zero-field behavior, $\langle^{2h}J_{Cl-N}\rangle$ decreases in the ground vibrational state to −12.1 Hz in ClH:NH$_3$ and −12.3 Hz in ClD:NH$_3$. These changes correlate with the increase in the expectation value of the Cl−N distance in the ground state relative to the equilibrium distance, as seen in Table 1 and Figure 4. In the excited dimer states, the expectation value of the Cl−N distance further increases, and $\langle^{2h}J_{Cl-N}\rangle$ decreases relative to the ground state. In the first-excited state of the proton-stretching mode, the expectation value of the Cl−N distance increases dramatically relative to the ground state, and there is a corresponding large decrease in $\langle^{2h}J_{Cl-N}\rangle$ from −12.1 to −9.7 Hz in ClH:NH$_3$ and from −12.3 to −10.1 Hz in ClD:NH$_3$.

There is an apparent anomaly in the ClH:NH$_3$ Cl−N coupling constants for the $\upsilon = 3$ excited state of the dimer-stretching mode and the first excited state of the proton-stretching mode at a field strength of 0.0055 au. It would be expected that $\langle^{2h}J_{Cl-N}\rangle$ should decrease as the dimer excited states increase in energy, and the Cl−N distance increases. However, the $\upsilon =$ 2 and 3 states of the dimer stretching mode have essentially identical Cl−N coupling constants of −10.40 and −10.38 Hz, respectively. Moreover, $\langle^{2h}J_{Cl-N}\rangle$ for the first excited state of the proton-stretching mode is only −9.69 Hz, whereas a larger value may have been anticipated. It would be tempting to interchange the assignments of these states. However, as noted above, the $\upsilon = 1$ state of the proton-stretching mode is in Fermi resonance with the $\upsilon = 3$ state of the dimer-stretching mode. A similar effect is observed for ClD:NH$_3$, although, in this case, the $\upsilon = 1$ state of the proton stretch is in Fermi-resonance with the $\upsilon = 2$ state of the dimer stretch.

At a field strength of 0.0150 au, the nature of the changes in $\langle^{2h}J_{Cl-N}\rangle$ as a function of vibrational state resemble those observed at zero-field. At this field strength, the hydrogen bond has ion-pair character, and as can be seen from Table 1, the expectation values of the Cl−N distance in the ground vibrational state are shorter than the equilibrium distance. $^{2h}J_{Cl-N}$ evaluated at the equilibrium geometry is −8.2 Hz, whereas $\langle^{2h}J_{Cl-N}\rangle$ in the ground vibrational state is −9.5 and −9.1 Hz for ClH:NH$_3$ and ClD:NH$_3$, respectively. Thus, the coupling constants increase as the Cl−N distance decreases from 3.004 to 2.988 and 2.996 Å, respectively. In the excited states of the dimer stretching mode, $\langle^{2h}J_{Cl-N}\rangle$ decreases further. In contrast, $\langle^{2h}J_{Cl-N}\rangle$ for the first excited state of the proton-stretching mode increases as the expectation value of the Cl−N distance decreases.

The calculation of $\langle^{2h}J_{Cl-N}\rangle$ for the ground state (that is, $\langle^{2h}J_{Cl-N}\rangle_{0,0}$) requires that both the vibrational wave function for this state and the coupling constant surface are available. Is it

TABLE 4: Ground State Expectation Values ($\langle {}^{2h}J_{Cl-N}\rangle_{0,0}$, Hz) and Thermally Averaged Cl−N Coupling Constants ($\langle {}^{2h}J_{Cl-N}\rangle_T$, Hz) for ClH:$NH_3$ and ClD:NH_3 at Various Field Strengths

	ClH:NH_3	ClD:NH_3
	Field = 0.0000 au	
$\langle {}^{2h}J_{Cl-N}\rangle_{0,0}$	−7.5	−6.9
$\langle {}^{2h}J_{Cl-N}\rangle_{100}$	−7.49	−6.93
$\langle {}^{2h}J_{Cl-N}\rangle_{150}$	−7.44	−6.89
$\langle {}^{2h}J_{Cl-N}\rangle_{200}$	−7.37	−6.85
$\langle {}^{2h}J_{Cl-N}\rangle_{298}$	−7.23	−6.75
	Field = 0.0055 au	
$\langle {}^{2h}J_{Cl-N}\rangle_{0,0}$	−12.1	−12.3
$\langle {}^{2h}J_{Cl-N}\rangle_{100}$	−12.1	−12.3
$\langle {}^{2h}J_{Cl-N}\rangle_{150}$	−12.1	−12.3
$\langle {}^{2h}J_{Cl-N}\rangle_{200}$	−12.0	−12.2
$\langle {}^{2h}J_{Cl-N}\rangle_{298}$	−11.9	−12.0
	Field = 0.0150 au	
$\langle {}^{2h}J_{Cl-N}\rangle_{0,0}$	−9.4	−9.1
$\langle {}^{2h}J_{Cl-N}\rangle_{100}$	−9.4	−9.1
$\langle {}^{2h}J_{Cl-N}\rangle_{150}$	−9.4	−9.0
$\langle {}^{2h}J_{Cl-N}\rangle_{200}$	−9.4	−9.0
$\langle {}^{2h}J_{Cl-N}\rangle_{298}$	−9.3	−8.9

possible to estimate $\langle {}^{2h}J_{Cl-N}\rangle_{0,0}$ for ClH:NH_3 and ClD:NH_3 by doing single-point calculations at the geometries corresponding to the expectation values of the ground-state Cl−N and Cl−H distances? For complexes with traditional and ion-pair hydrogen bonds, the data of Table 3 suggest that this is a reasonable approach. At fields of 0.0000 and 0.0150 au, the values of ${}^{2h}J_{Cl-N}$ from single-point calculations for the complexes with traditional and ion-pair hydrogen bonds differ from $\langle {}^{2h}J_{Cl-N}\rangle_{0,0}$ by less than 0.2 Hz. However, $\langle {}^{2h}J_{Cl-N}\rangle_{0,0}$ for the proton-shared complex at 0.0055 au is overestimated by the single-point calculations by 0.9 Hz for ClH:NH_3 and 0.5 Hz for ClD:NH_3. This difference is due to the increased delocalization of the ground-state wave function at 0.0055 au compared to 0.0000 and 0.0150 au fields, as evident from Figure 1. Nevertheless, this approach seems encouraging, and provides a better estimate of $\langle {}^{2h}J_{Cl-N}\rangle_{0,0}$ than a single-point calculation of ${}^{2h}J_{Cl-N}$ at the equilibrium geometry.

Ground State and Thermally Averaged Coupling Constants. In recent experimental studies, coupling constants across hydrogen bonds have been measured as a function of temperature in the range from 100 to 200 K.[1,8] How does thermal vibrational averaging effect coupling constants? Table 4 reports thermal averages of $\langle {}^{2h}J_{Cl-N}\rangle$ at 100, 150, 200, and 298 K for ClH:NH_3 and ClD:NH_3 at field strengths of 0.0000, 0.0055, and 0.0150 au. Also given for comparison are the expectation values of the coupling constants in the ground vibrational state, $\langle {}^{2h}J_{Cl-N}\rangle_{0,0}$. At zero-field, $\langle {}^{2h}J_{Cl-N}\rangle_{0,0}$ for ClH:NH_3 is −7.5 Hz. The thermally averaged values at 100, 150, 200, and 298 K are −7.5, −7.4, −7.4, and −7.2 Hz, respectively. Similarly, $\langle {}^{2h}J_{Cl-N}\rangle_{0,0}$ for ClD:NH_3 is −6.9 Hz, and the thermally averaged values at the four temperatures are −6.9, −6.9, -6.9, and −6.8 Hz, respectively. Thus, over this temperature range, thermally averaged coupling constants differ at most by 0.3 Hz from ground-state values.

At a field of 0.0055 au, where the hydrogen bond is proton-shared, the thermally averaged coupling constants at 100, 150, 200, and 298 K are again similar to ground-state values. At a field of 0.0150 au, the hydrogen bond is an ion-pair hydrogen bond, and thermal averaging of $\langle {}^{2h}J_{Cl-N}\rangle$ over the temperature range from 100 to 300 K yields coupling constants that are very close to $\langle {}^{2h}J_{Cl-N}\rangle_{0,0}$. Thus, these results suggest that thermal averaging over the vibrational states at temperatures below 300 K has little effect on coupling constants for either ClH:NH_3 or ClD:NH_3, regardless of hydrogen bond type.

TABLE 5: Cl−N Spin−Spin Coupling Constants (${}^{2h}J_{Cl-N}$, Hz) for Equilibrium Structures of ClH:NH_3 as a Function of Field Strength (au)[a]

field	explicit ${}^{2h}J_{Cl-N}$[b]	implicit ${}^{2h}J_{Cl-N}$[c]
0.0000	−5.9	−5.9
0.0010	−6.6	−6.3
0.0025	−7.8	−7.1
0.0040	−9.3	−8.2
0.0055	−13.5	−12.2
0.0100	−10.9	−9.5
0.0150	−8.2	−7.0

[a] Data taken from ref 21. [b] Computed using the optimized geometry (R_e) for each complex at the indicated field strength, in the presence of the field. [c] Computed using the optimized geometry (R_e) for each complex at the indicated field strength but at zero external field.

${}^{2h}J_{Cl-N}$ Computed With and Without an External Field. Table 5 reports implicit and explicit single-point coupling constants (${}^{2h}J_{Cl-N}$) for the equilibrium structures of ClH:NH_3.[21] The implicit coupling constants are computed in the absence of the external field, but at equilibrium geometries obtained in the presence of the field. Explicit coupling constants are calculated at the optimized geometry at a given field strength, in the presence of the external field. It is apparent from Table 5 that, although explicit coupling constants are always greater than implicit at a given field strength, their variation with field strength is the same. That is, ${}^{2h}J_{Cl-N}$ initially increases as the field strength increases, exhibits a maximum at a field of 0.0055 au when the hydrogen bond is proton-shared and close to quasisymmetric, and then decreases as the hydrogen bond assumes greater ion-pair character. Nevertheless, implicit and explicit values of ${}^{2h}J_{Cl-N}$ for the equilibrium structures are different, and the differences are larger at higher fields. Therefore, it is appropriate to investigate how coupling constants computed from the property surfaces obtained at different fields compare with those obtained from the zero-field surface.

Computed explicit and implicit single-point values of ${}^{2h}J_{Cl-N}$ evaluated at the equilibrium geometries and at the geometries defined by the expectation values of the Cl−N and Cl−H distances in the ground vibrational states and expectation values ($\langle {}^{2h}J_{Cl-N}\rangle$) for the ground and selected excited vibrational states of ClH:NH_3 and ClD:NH_3 are reported in Table 3. Implicit values are given in parentheses. A comparison of corresponding single-point and expectation values shows that implicit coupling constants underestimate explicit by 1.3−1.5 Hz at a field of 0.0055 au. At 0.0150 au, the differences are greater, ranging from 1.0 to 1.6 Hz for the equilibrium, ground state, and excited dimer vibrational states and to 2.8 and 2.4 Hz for the first excited state of the proton-stretching mode of ClH:NH_3 and ClD:NH_3, respectively. Implicit ground-state expectation values underestimate explicit values by 1.4 Hz for the proton-shared structures at 0.0055 au and by 1.6 and 1.5 Hz for the ion-pair structures of ClH:NH_3 and ClD:NH_3, respectively, at 0.0150 au. These differences are significant, particularly if computed coupling constants are to be used to extract intermolecular distances. Thus, if coupling constants are computed for structures produced by an external field, they should be evaluated in the presence of the field.

Isotope Effects. Isotope effects on spin−spin coupling constants have been observed experimentally.[35,36] These effects are a result of changes in the vibrational wave functions on deuteration and accompanying changes in Cl−N and Cl−H (Cl-D) distances. Table 1 presents equilibrium and ground-state expectation values of the Cl−N and Cl−H (Cl−D) distances

for both ClH:NH_3 and ClD:NH_3 at each field strength considered. Table 3 presents single-point and expectation values of coupling constants. At zero-field, there is a significant difference between the ground-state expectation values of the Cl−N distances in the two isotopomers, with the Cl−N distance in ClH:NH_3 being 0.025 Å shorter. As a result, $\langle {}^{2h}J_{Cl-N}\rangle_{0,0}$ for ClH:NH_3 is 0.6 Hz greater than for ClD:NH_3. From Table 3, it can be seen that at zero-field the change in $\langle {}^{2h}J_{Cl-N}\rangle$ on deuteration is greatest in the ground state, but as the excited-state energy increases, $\langle {}^{2h}J_{Cl-N}\rangle$ for the two isotopomers becomes similar. The relatively large isotope effect in the ground state may not be typical for isotopomers with traditional hydrogen bonds but may be a consequence of the particular nature of the ClH:NH_3 potential surface.

The isotope effect on $\langle {}^{2h}J_{Cl-N}\rangle_{0,0}$ is not as great for the proton-shared complex at 0.0055 au or the ion-pair complex at 0.0150 au. For the proton-shared complex at 0.0055 au, isotopic substitution of D for H increases $\langle {}^{2h}J_{Cl-N}\rangle_{0,0}$ by only 0.2 Hz, from −12.1 Hz in ClH:NH_3 to −12.3 Hz in ClD:NH_3. This change does not correlate with the ground-state expectation value of the Cl−N distance in the two isotopomers, which is 0.008 Å greater in ClD:NH_3 than in ClH:NH_3. This difference may be a consequence of the delocalized nature of the ground-state wave functions at this field strength. The single-point values of ${}^{2h}J_{Cl-N}$ at the ground-state geometries for the two isotopomers are greater for ClH:NH_3, as expected. In contrast, at a field of 0.0150 au, isotopic substitution decreases $\langle {}^{2h}J_{Cl-N}\rangle_{0,0}$ by 0.4 Hz in the ion-pair complex, from −9.5 Hz in ClD:NH_3 to −9.1 Hz in ClD:NH_3. This changes correlates with an increase of 0.008 Å in the expectation value of the Cl−N distance in the ground state of ClD:NH_3 compared to ClH:NH_3. Thus, whether $\langle {}^{2h}J_{Cl-N}\rangle_{0,0}$ increases or decreases upon deuteration depends on hydrogen bond type.

Conclusions

The results of this study of two-bond Cl−N coupling constants (${}^{2h}J_{Cl-N}$ and $\langle {}^{2h}J_{Cl-N}\rangle$) in ClH:$NH_3$ and ClD:NH_3 are the basis for proposing the following answers to the questions raised in the Introduction.

1. As noted previously in many studies, coupling constants exhibit maximum absolute values in complexes with proton-shared hydrogen bonds.

2. Single-point values of the coupling constant, ${}^{2h}J_{Cl-N}$, can be significantly different when computed at the equilibrium geometry and at the geometry defined by the expectation values of the coordinates for the ground vibrational state. These values also differ from the calculated ground-state expectation values, $\langle {}^{2h}J_{Cl-N}\rangle_{0,0}$. For ClH:$NH_3$ and ClD:NH_3, equilibrium ${}^{2h}J_{Cl-N}$ and $\langle {}^{2h}J_{Cl-N}\rangle_{0,0}$ differ by about 1−1.5 Hz. For complexes with traditional and ion-pair hydrogen bonds, the absolute values of $\langle {}^{2h}J_{Cl-N}\rangle_{0,0}$ are greater than the equilibrium values of ${}^{2h}J_{Cl-N}$, whereas for complexes with proton-shared hydrogen bonds, the equilibrium values are greater. These results suggests that coupling constants should be evaluated as ground-state expectation values, whenever possible. A single-point calculation to determine ${}^{2h}J_{Cl-N}$ at the geometry defined by the expectation values of the coordinates in the ground state may or may not reproduce $\langle {}^{2h}J_{Cl-N}\rangle_{0,0}$, depending on hydrogen bond type. However, such single-point values of ${}^{2h}J_{Cl-N}$ are much closer to $\langle {}^{2h}J_{Cl-N}\rangle_{0,0}$ than are single-point values calculated at the equilibrium geometry.

3. Thermal averaging of $\langle {}^{2h}J_{Cl-N}\rangle$ over excited vibrational states at temperatures below 300 K has little effect, because the thermally averaged coupling constants are essentially the same as $\langle {}^{2h}J_{Cl-N}\rangle_{0,0}$ for both ClH:NH_3 and ClD:NH_3.

4. Coupling constants evaluated for ClH:NH_3 and ClD:NH_3 at a given geometry as explicit functions of the strength of an external field are always greater than those evaluated as implicit functions at zero-field. An external field changes not only the potential surface but also the coupling constant surface. Coupling constants computed for a structure produced by an external field should be evaluated in the presence of the field (explicit ${}^{2h}J_{Cl-N}$).

5. The effect of isotopic substitution of D for H on $\langle {}^{2h}J_{Cl-N}\rangle_{0,0}$ shows some dependence on hydrogen bond type. The most dramatic effect is observed for the traditional hydrogen bond, in which case isotopic substitution decreases $\langle {}^{2h}J_{Cl-N}\rangle_{0,0}$ by 0.6 Hz. Substitution of D for H also decreases $\langle {}^{2h}J_{Cl-N}\rangle_{0,0}$ in the complex with an ion-pair hydrogen bond, but by only 0.4 Hz. $\langle {}^{2h}J_{Cl-N}\rangle_{0,0}$ for the complex with a proton-shared hydrogen bond increases by 0.3 Hz in ClD:NH_3 relative to ClH:NH_3. This suggests that the change in ${}^{2h}J_{X-Y}$ upon isotopic substitution may be useful for differentiating traditional and proton-shared hydrogen bonds.

The generality of these observations will be tested in future studies of coupling constants in other hydrogen-bonded systems.

Acknowledgment. This work was supported by the National Science Foundation (Grant CHE-9873815) and the Australian Reseach Council (Grant A2543). This support and the support of the Ohio Supercomputer Center are gratefully acknowledged.

References and Notes

(1) Shenderovich, I. G.; Smirnov, S. N.; Denisov, G. S.; Gindin, V. A.; Golubev, N. S.; Dunger, A.; Reibke, R.; Kirpekar, S.; Malkina, O. L.; Limbach, H.-H. *Ber. Bunsen-Ges. Phys. Chem.* **1998**, *102*, 422.

(2) Laynez, J.; Menéndez, M.; Velasco, J. L. S.; Llamas-Saiz, A. L.; Foces-Foces, C.; Elguero, J.; Molina, P.; Alajarín, M. *J. Chem. Soc., Perkins Trans. 2* **1993**, 709.

(3) Dingley, A. J.; Masse, J. E.; Peterson, R. D.; Barfield, M.; Feigon, J.; Grzesiek, S. *J. Am. Chem. Soc.* **1999**, *121*, 6019.

(4) Scheurer, C.; Brüschweiler, R. *J. Am. Chem. Soc.* **1999**, *121*, 8661.

(5) Golubev, N. S.; Shenderovich, I. G.; Smirnov, S. N.; Denisov, G. S.; Limbach, H.-H. *Chem. Eur. J.* **1999**, *5*, 492.

(6) Golubev, N. S.; Denisov, G. S.; Smirnov, S. N.; Shehepkin, D. N.; Limbach, H.-H. *Z. Phys. Chem.* **1996**, *196*, 73.

(7) Smirnov, S. N.; Golubev, N. S.; Denisov, G. S.; Benedict, H.; Schah-Mohammedi, P.; Limbach, H.-H. *J. Am. Chem. Soc.* **1996**, *118*, 4094.

(8) Smirnov, S. N.; Benedict, H.; Golubev, N. S.; Denisov, G. S.; Kreevoy, M. M.; Schowen, R. L.; Limbach, H.-H. *Can. J. Chem.* **1999**, *77*, 943.

(9) Benedict, H.; Shenderovich, I. G.; Malkina, O. L.; Malkin, V. G.; Denisov, G. S.; Golubev, N. S.; Limbach, H.-H. *J. Am. Chem. Soc.* **2000**, *122*, 1979.

(10) Pecul, M.; Leszczynski, J.; Sadlej, J. *J. Phys. Chem. A* **2000**, *104*, 8105.

(11) Barfield, M.; Dingley, A. J.; Feigon, J.; Grzesiek, S. *J. Am. Chem. Soc.* **2001**, *123*, 4014.

(12) Dingley, A. G.; Grzesiek, S. *J. Am. Chem. Soc.* **1998**, *120*, 8293.

(13) Pecul, M.; Sadlej, J. Leszczynski, J. *J. Chem. Phys.* **2001**, *115*, 5498.

(14) Czernek, J.; Bruschweiler, R. *J. Am. Chem. Soc.* **2001**, *123*, 11079.

(15) Perera, S. A.; Bartlett, R. J. *J. Am. Chem. Soc.* **2000**, *122*, 1231.

(16) Del Bene, J. E.; Perera, S. A.; Bartlett, R. J. *J. Am. Chem. Soc.* **2000**, *122*, 3560.

(17) Del Bene, J. E.; Jordan, M. J. T. *J. Am. Chem. Soc.* **2000**, *122*, 4794.

(18) Del Bene, J. E.; Perera, S. A.; Bartlett, R. J.; Alkorta, I.; Elguero, J. *J. Phys. Chem. A.* **2000**, *104*, 7165.

(19) Del Bene, J. E.; Bartlett, R. J. *J. Am. Chem. Soc.* **2000**, *122*, 10480.

(20) Del Bene, J. E.; Perera, S. A.; Bartlett, R. J. *J. Phys. Chem. A* **2001**, *105*, 930.

(21) Chapman, K.; Crittenden, D.; Bevitt, J.; Jordan, M. J. T.; Del Bene, J. E. *J. Chem. Phys. A* **2001**, *105*, 5442.

(22) Del Bene, J. E.; Perera, S. A.; Bartlett, R. *J. Magn. Reson. Chem.* **2001**, *39*, S109.

(23) Del Bene, J. E.; Jordan, M. J. T.; Perera, S. A.; Bartlett, R. J. *J. Phys. Chem. A* **2001**, *105*, 8399.

(24) Jordan, M. J. T.; Del Bene, J. E. *J. Am. Chem. Soc.* **2000**, *122*, 2101.

(25) Bartlett, R. J.; Silver, D. M. *J. Chem. Phys.* **1975**, *62*, 3258.
(26) Bartlett, R. J.; Purvis, G. D. *Int. J. Quantum Chem.* **1978**, *14*, 561.
(27) Pople, J. A.; Binkley, J. S.; Seeger, R. *Int. J. Quantum Chem. Quantum Chem. Symp.* **1976**, *10*, 1.
(28) Krishnan, R.; Pople, J. A. *Int. J. Quantum Chem.* **1978**, *14*, 91.
(29) Dunning, T. H., Jr. *J. Chem. Phys.* **1989**, *90*, 1007.
(30) Woon, D. E.; Dunning, T. H., Jr. *J. Chem. Phys.* **1995**, *103*, 4572.
(31) Bevitt, J.; Chapman, K.; Crittenden, D.; Jordan, M. J. T.; Del Bene, J. E. *J. Phys. Chem. A* **2001**, *105*, 3371.
(32) Perera, S. A.; Nooijen, M.; Bartlett, R. *J. Chem. Phys.* **1996**, *104*, 3290.
(33) Schäfer, A.; Horn, H.; Ahlrichs, R. *J. Chem. Phys.* **1992**, *97*, 2571.
(34) ACES II is a program product of the Quantum Theory Project, University of Florida. Authors: Stanton, J. F.; Gauss, J.; Watts, J. D.; Nooijen, M.; Oliphant, N.; Perera, S. A.; Szalay, P. G.; Lauderdale, W. J.; Gwaltney, S. R.; Beck, S.; Balkova, A.; Bernholdt, D. E.; Baeck, K.-K.; Tozyczko, P.; Sekino, H.; Huber, C.; Bartlett, R. J. Ingetral packages included are VMOL (Almlof, J.; Taylor, P. R.); VPROPS (Taylor, P. R.); ABACUS (Helgaker, T.; Jensen, H. J. Aa.; Jorgensen, P.; Olsen, J.; Taylor, P. R.). Brillouin-Wigner perturbation theory was implement by Pittner, J.
(35) Benedict, H.; Limbach, H.-H.; Wehlan, M.; Fehlhammer, W.-P.; Golubev, N. S.; Janoschek, R. *J. Am. Chem. Soc.* **1998**, *120*, 2939.
(36) Schah-Mohammedi, P.; Shenderovich, I. G.; Detering, C.; Limbach, H.-H.; Tolstoy, P. M.; Smirnov, S. N.; Denisov, G. S.; Golubev, N. S. *J. Am. Chem. Soc.* **2000**, *122*, 12878.